

STM tunneling spectroscopic studies of $\text{YNd}_x\text{Ba}_{2-x}\text{Cu}_3\text{O}_{7-\delta}$ thin filmsM. Iavarone,^{1,2} M. Salluzzo,¹ R. Di Capua,¹ M. G. Maglione,¹ R. Vaglio,¹ G. Karapetrov,² W. K. Kwok,² and G. W. Crabtree²¹*INFN–University of Naples Federico II, Dipartimento di Scienze Fisiche, Piazzale Tecchio 80, 80125 Naples, Italy*²*Materials Science Division, Argonne National Laboratory, 9700 South Cass Avenue, Argonne, Illinois 60439*

(Received 13 June 2001; published 22 May 2002)

We performed tunneling spectroscopy on high quality superconducting $\text{YNd}_x\text{Ba}_{2-x}\text{Cu}_3\text{O}_{7-\delta}$ thin films using a low-temperature scanning tunneling microscope. Superconducting regions show very well-defined gap structures. Disorder introduced by Nd substitution at the Ba site dramatically affects locally the quasiparticle density of states. The measurements show that the impurities induce surface resonant states at energies very close to the Fermi energy, typical of a *d*-wave superconductor.

DOI: 10.1103/PhysRevB.65.214506

PACS number(s): 74.76.Bz, 68.37.Ef, 68.55.Ln

Impurity states in superconductors provide a wealth of information on the pairing symmetry and mechanism through the local density of states and its spatial variation. Special attention has been given to nonmagnetic impurities that affect the local order parameter in conventional superconductors only weakly but are strong pair breakers for the higher orbital momentum states of *d*-wave superconductors.^{1–3} Scanning tunneling spectroscopy is an ideal tool to examine the local density of states (LDOS) in the superconducting state with high spatial and energy resolution. Recently impurity scattering studies have been performed in Nb (Ref. 4) and $\text{Bi}_2\text{Sr}_2\text{CaCu}_2\text{O}_{8+\delta}$ (BSCCO) (Refs. 5–7) single crystals. For nonmagnetic impurities in Nb no effects on the LDOS was observed, whereas in BSCCO single-crystals quasiparticle resonances at low energies were found at the impurity site, a clear evidence for unconventional pairing mechanism.

Although systematic scanning tunneling studies have been carried out on BSCCO single crystals^{8–10} and some recent measurements have also been reported for BSCCO thin films,¹¹ scanning tunneling microscope (STM) technique has proven more challenging for $\text{YBa}_2\text{Cu}_3\text{O}_{7-\delta}$ (YBCO) (Ref. 12) due to difficulties with surface preparation. Tunneling spectroscopy over a single oxygen vacancy in the Cu-O chain of YBCO single crystals has been reported¹³ and quasiparticle scattering states have been recently reported for YBCO both in form of thin films and single crystal.^{14,15}

In this paper we present a report on scanning tunneling spectroscopy studies of $\text{YNd}_x\text{Ba}_{2-x}\text{Cu}_3\text{O}_{7-\delta}$ (YNBCO) thin films. This system is very similar to YBCO with exception that Nd substitution in Ba site introduces quasiparticle scattering centers. The observed scanning tunneling spectroscopy (STS) spectra far away from the impurity site are quite similar to YBCO spectra reported earlier^{12,16} whereas the spectra near impurities show a pronounced resonance at energy close to the Fermi level. This signature in the tunneling spectra has been predicted to be an evidence of unitary limit scattering in *d*-wave superconductors.

YNBCO films have been deposited by high-pressure oxygen dc sputtering.¹⁷ The planar targets used for the deposition had composition $\text{Y}_1\text{Nd}_{0.1}\text{Ba}_{1.9}\text{Cu}_3\text{O}_7$. The films were deposited on LaAlO_3 or SrTiO_3 (100) substrates at high pressures ranging between 1.4 and 2.0 Torr. A deposition tem-

perature of about 850 °C and a total pressure of 1.6 Torr produced the best films. The gas mixture was composed mainly of pure O_2 with a small percentage of Ar (about 5%). After the deposition the oxygen pressure was increased to 400 Torr and the substrate temperature was gradually reduced to 500 °C over 30 min. Finally, the films were annealed at 500 °C in 400 Torr of partial oxygen pressure for 1 h. After the deposition the samples chosen for the STM measurements were transferred at a pressure lower than 10^{-7} Torr to a fast-entry introchamber where the samples were hermetically sealed in a glass container filled with ultrahigh purity Ar gas.

θ - 2θ x-ray spectra showed that the films are *c* axis oriented with a full width at half maximum (FWHM) of the (001) rocking curve less than 0.08° .¹⁷ These values were routinely obtained and reveal high structural quality of the samples. The maximum superconducting critical temperature T_c achieved was about 86 K with a transition width lower than 1 K. The amount of Nd excess, estimated by energy dispersive x-ray analysis (EDX) in combination with x-ray simulations of the measured spectra, was about 3–4% in YNBCO optimized films. In particular the systematic changes of the *c*-axis peak intensity and position in the θ - 2θ x-ray spectra with Nd doping cannot be explained by possible substitution of Nd at the Y site or by oxygen underdoping. Indeed the *c* axis of each YNBCO sample is always shorter than the *c* axis of optimally doped YBCO films, while both Nd substitution at the Y site and oxygen deficiency would increase the *c* axis [the $\text{NdBa}_2\text{Cu}_3\text{O}_{7-\delta}$ (NBCO) unit cell is 11.75 Å long]. Also the relative change of the peak intensity ratios $I(005)/I(007)$ and $I(006)/I(007)$ is in qualitative agreement with a partial substitution of Nd at Ba sites.

The room-temperature resistivity of a typical YNBCO film obtained by a four-point probe technique gives a value of 80 $\mu\Omega$ cm, which is comparable to that of a typical YBCO film. The nonzero value of the intercept resistance at $T=0$, indicates the existence of a residual scattering rate due to impurities. The impurities could be related to the Nd substitution of Ba, since stoichiometric YBCO thin films,¹⁸ grown in the same preparation system under identical growth conditions, show zero residual resistivity. Third-harmonic inductive measurements, show a critical current density J_c of 3.5×10^7 A/cm² at 4.2 K. Finally, Hall effect measurements at

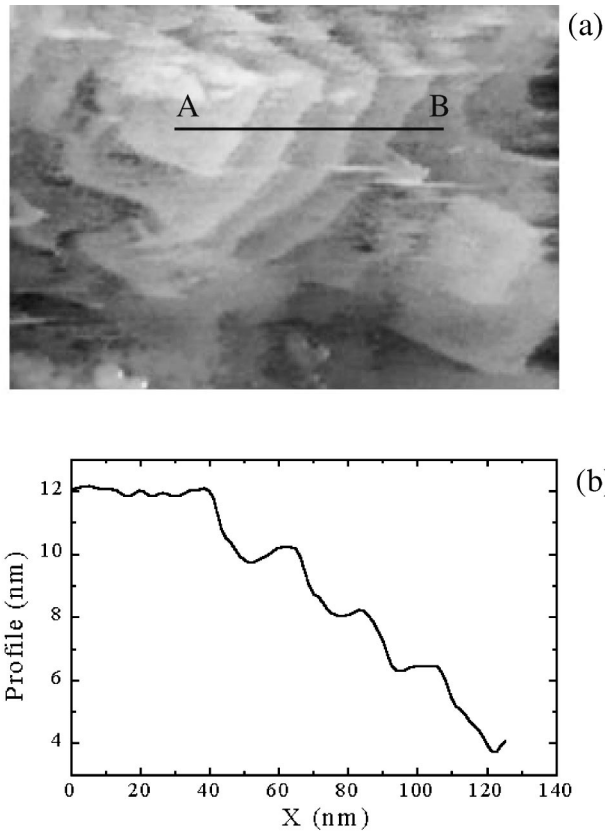


FIG. 1. (a) Topographic image of a YNBCO thin-film surface at $T=4.2$ K obtained in the constant current mode. The scan area is 300, 200 nm and the imaging parameters are $I=100$ pA and $V=-1$ V; (b) Profile of the section AB shown in Fig. 1(a).

100 K reveal that the samples are underdoped with number of carriers about $2 \times 10^{22} \text{ cm}^{-3}$.

We performed our experiment using a home made low-temperature STM operating at 4.2 K in helium exchange gas. We used electrochemically etched Pt-Ir tips. The measurements were performed on as-grown thin films, which were kept in inert atmosphere before the experiment.

STM topographic images, as reported in Fig. 1, show surfaces characterized by terraces having step height equal to either one or two c -axis lattice parameters.

The current-voltage (I - V) spectra were recorded at different locations on the sample surface by sweeping the bias voltage of the sample while the tip-sample distance was kept constant in the open loop condition. The LDOS of the YNBCO thin-film surface was obtained by measuring the differential conductance dI/dV vs V of the tunneling sample-tip junction with a standard lock-in technique. Typical modulation frequencies were ~ 0.3 – 1 kHz and ac modulations amplitude ~ 0.4 – 1 mV. Assuming that the tip DOS is constant close to the Fermi energy in first approximation the differential conductance is proportional to the sample DOS smeared by the thermal factor $\sim kT$. All the measurements were carried out on the (001) surface of as-grown films.

In order to achieve reproducible spectroscopy we required the tunneling current to pass several tests. The only spectra that we will present show the following features: (a) tempo-

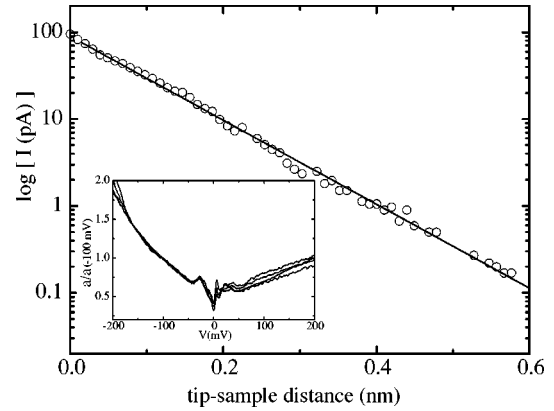


FIG. 2. Variation of the tunneling current I as a function of the tip-sample distance d . The circles represent the experimental data while the solid curve is the result of an exponential fit giving $\Phi = 0.9$ eV. In the inset are reported the conductance curve, normalized at $V = -100$ mV, measured at 4.2 K for different values of the tunneling resistance ranging between 1 and 3 G Ω .

ral reproducibility of topographic images; (b) temporal reproducibility of the spectra; (c) reproducible spectra as a function of the tunneling resistance. Another important check of the junction quality is the exponential decay of the tunneling current as a function of the tip-sample distance. In Fig. 2 a typical tunneling current dependence as a function of the electrode separation is reported. The exponential fit of the experimental curve $I = I_0 \exp(-1.025\sqrt{\Phi}d)$, where d is the tip-sample distance, gives an apparent work function $\Phi = 0.9$ eV, which is a clear signature of a clean vacuum tunneling. All the measurements presented in this paper have been observed in correspondence of an apparent work function higher than 0.9 eV. Our tunneling spectra are independent on the tip-sample separation as demonstrated in the inset of Fig. 2, where several dI/dV curves are shown, recorded at junction resistances ranging between 1 and 3 G Ω .

Figure 3 shows the essential features of superconducting LDOS at 4.2 K, in zero magnetic field, obtained at different locations on the film surface, far from Nd impurity sites.

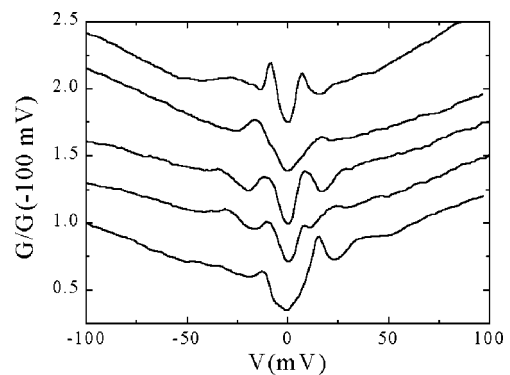


FIG. 3. Conductance spectra recorded at 4.2 K at various location on the surface of two YNBCO thin film having similar doping and critical temperature 86 K. For all of them the tunneling resistance is 1 G Ω .

These data are qualitatively similar to those obtained previously from STM measurements¹² and from planar junctions by Valles *et al.*¹⁶ on YBCO single crystals. We observe two gaplike features. The main one corresponds to a broad peak at 20–30 meV. The second one appears at low energies in the range of 5–10 meV. The sharpness of the second feature varies depending on the location on the surface. When the low-energy feature is pronounced it appears as a peak in the spectrum while the high-energy feature appears broad. In contrast, when the low-energy feature appears weaker it forms a shoulder in the larger gap structure. This subgap structure is found consistently and is more pronounced and robust than in STM measurements reported on YBCO earlier.¹² Similar peaks at the above energies were also observed in planar junctions as well as in YBCO and Pr-doped YBCO single crystals.^{19,20} It was hypothesized that the double gap structure could arise from the anisotropy of the in-plane and out-of-plane values of the superconducting gap or from a proximity effect between the planes and the chain.¹⁶ According to the anisotropy picture the structures at 5–10 meV and the 20–25 meV can be associated with energy gaps along the c axis and in the a - b plane, respectively. This explanation can be ruled out for our spectra, because by tunneling along the c axis the tunneling current probes only the a - b plane DOS, due to the two-dimensional character of the Fermi surface in HTc materials. In the proximity-coupled picture the small gap arises from the Cu-O chains, which are driven superconducting by proximity to the planes which are less than 1 nm away. Since we could not obtain atomic resolution (which seems to be achievable only for cold cleaved YBCO single crystals^{21,22}) we could not identify the top layer from STM images. Therefore it remains unclear why in some regions the low-energy feature is very well defined [as in curve (a) in Fig. 3]. Our data are also consistent with a chain gap driven by a charge-density wave scenario, as suggested by De Lozanne.²²

The zero-bias conductance in all our measurements ranges between 50 and 70% of the conductance value at 100 meV. This relatively high value of zero-bias conductance has been reported often in literature^{12,13,16,19,20} suggesting it could be an intrinsic property of the material. The background of the spectra always increases when moving away from E_F , and it also varies from one location to another. Background with both V shape and asymmetric V shape were observed. This asymmetry about the zero bias is a common feature of the tunneling spectra obtained on YBCO and NBCO single crystals.²³ The conductance is stronger at negative sample bias voltages (electron tunneling from filled states of the sample to empty states in the tip) at some locations, and weaker at other locations. This result is in contrast to what has been reported for BSCCO single crystals where the asymmetry of the spectra is always the same.^{8–10}

At some locations the LDOS of the YNBCO surface is strongly modified and a peak occurs at energies Ω_0 close to but always below E_F , similar to the peak reported in BSCCO single crystals with Zn impurities.⁵ On average, the spectra of the films studied has $\Omega_0 = -1.7 \pm 0.4$ meV, with FWHM of 4 meV. Spectra with these midgap states are clustered within distances of about 2–4 nm of each other. In Fig.

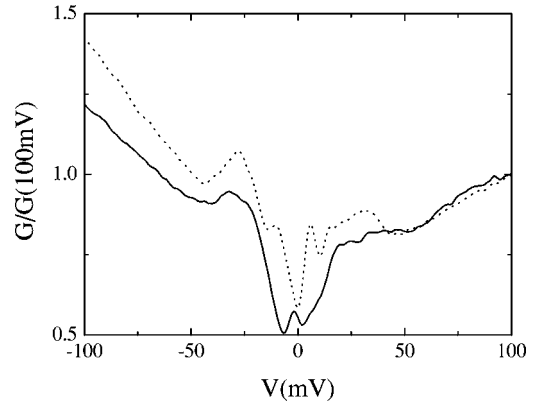


FIG. 4. Two conductance curve recorded 4 nm apart on a YNBCO thin-film surface: Both curves have been recorded at 4.2 K and correspond to a tunneling resistance of 1 G Ω .

4 a spectrum recorded at one of these locations is reported together with one recorded 4 nm away. We interpret these midgap states as due to Nd impurities. The impurity affects not only the subgap region of the DOS, but also the width of the superconducting gap, as shown in Fig. 4.

According to theoretical models a nonmagnetic impurity in a d wave superconductor will give rise to a bound excitation at energy $\Omega_0 < \Delta_0$, where Δ_0 is the energy gap away from the impurity site. The midgap state energy Ω_0 is determined by the strength of the scattering potential, giving $\Omega_0 = E_F$ in the unitary limit. If the impurity scattering is close enough to the unitary limit, and for a gap function of $d_{x^2-y^2}$ symmetry at the Fermi surface, the strength of the scattering leads to low-energy excitations at energies given by³

$$\frac{\Omega_0}{\Delta_0} = \frac{\pi c}{2 \ln(8 \pi c)}$$

where Δ_0 is the energy gap far away from the impurity site, $c = \cot(\delta_0)$ and δ_0 is the phase shift of the superconducting order parameter due to the impurity scattering. Using an average gap $\Delta_0 = 20$ – 25 meV and $\Omega_0 = -1.7$ meV, we obtain a phase shift $\delta_0 = 0.46\pi$, which confirms that the scattering is very close to the unitary limit ($\delta_0 = \pi/2$). The resonance peak is expected to persist up to $c \rightarrow 1$ where it should appear very broad and it is expected to disappear for Born scattering ($c \gg 1$). According to this scenario the strength of the impurity-induced contribution is supposed to decay as $(\xi/r)^{-2}$ at large distances, where ξ is the superconducting coherence length, and is expected to follow spatially, around the impurity site, a fourfold symmetry of the DOS, aligned with the d -wave gap nodes. It is worth to outline in this context that a small s -wave component would be invisible in an STM experiment. We did not observe the cross-shape pattern of the spatial distribution of the bound states, predicted theoretically and observed experimentally in the case on Zn impurity in BSCCO single crystals.⁵ More detailed high-resolution spatial measurements are needed to address this issue.

The scattering resonances are observed far from morphological features, such as steps and grain boundaries, there-

fore, it is possible to exclude that structural disorder is responsible for such behavior. The density of the observed scattering resonance sites is about $x=4\%$ —in reasonable agreement with the percentage of Nd excess in YNBCO films, estimated by EDX analysis in combination with x-ray simulations of the measured spectra. Oxygen disorder is not unlikely since Nd excess at Ba site can indeed destroy the CuO chains. However, it is important to stress that resonance peaks close to the Fermi energy have never been observed in high quality YBCO films and crystals, and even in oxygen underdoped YBCO samples.²⁴ Finally, we would like to mention that the role of unitary scattering center of Nd ions at Ba site is perfectly in agreement with the low-temperature penetration depth measurements performed on NBCO films³¹ and recently on YNBCO films.²⁵ On the contrary it is well established that the role of oxygen deficiency is very different, since systematic measurements of the penetration depth of YBCO oxygen underdoped samples suggest, if any, only a very weak scattering from oxygen vacancies.²⁶ Preliminary STM measurements, performed on $\text{Nd}_{1+x}\text{Ba}_{2-x}\text{Cu}_3\text{O}_{7-\delta}$ (NBCO off) thin films, characterized by a larger percentage of Nd excess ($x=0.15$), show that the density of the resonance sites is correspondingly much higher. These results are in agreement with our interpretation of the excess Nd ions as quasiparticle scattering centers responsible for the observed resonances.

We also observe impurity-induced excitation near other kinds of pointlike defects on epitaxial film surfaces that could host midgap states.⁷ For example, some of the spectra recorded on the terrace steps show a zero bias conductance peak. In this case as already reported in the literature for STM/STS and other tunneling experiment the predominant *a-b* contribution to the tunneling current could be the origin of an Andreev bound state when the incident and the reflected quasiparticle experiences a sign change of the order parameter.²⁷

Resonance peaks close to the Fermi energy have not been observed in tunneling experiments using planar junctions on Pr-doped YBCO epitaxial thin films.^{19,20,28} This tunneling geometry measures an average spectrum where the impurity contribution is weighted by its concentration. Recent theoretical calculation for a simple random distribution of unitary impurities²⁹ show that at low impurity concentration the impurity spectral weight will be too small to be experimentally observed, while at high concentrations the impurity interactions increase the conductance value at zero-bias $G(0)$ without giving rise to a peak.

Our experiment raises interesting questions about the contrast between impurity-induced scattering in the YBCO and BSCCO system. The difference between our experiment and the BSCCO results reported earlier is that Zn is nonmagnetic

while a free Nd ion has a finite magnetic moment. The question is then what is the magnetic state of Nd in the Ba site and how the magnetic moment, if any, of the Nd substitute affects the impurity-induced quasiparticle states.

From the theoretical standpoint recent calculations for isolated magnetic impurities³⁰ find that the resonance peak splits into two due to the effective magnetic field. The question arises if this splitting is strong enough to be observable in STS experiments. In general, it is difficult to estimate the effective magnetic field. Moreover the situation is very different from the case of Zn impurity in BSCCO because in the latter case Zn is found to preferentially substitute for the Cu atoms, therefore, it provides a well controlled way of disturbing the CuO_2 planes that are believed to be the key element in all high- T_c superconductors. In YNBCO, on the other hand, Nd mainly substitutes for Ba and, therefore, the scattering center is outside the CuO_2 planes. We cannot rule out that Nd substitution at the Ba site may induce a free spin in the CuO plane by disordering the chains. Nevertheless *ab*-plane penetration depth measurements reported recently for epitaxial NBCO off thin films³¹ seem to quantitatively exclude this possibility showing a behavior that is very similar to the penetration depth measurements in YBCO single crystals in which Zn impurities are added to introduce disorder³² and, therefore, suggesting that Nd at the Ba site, at low impurity concentration, acts as a strong *nonmagnetic* impurity scattering center for the carriers in the CuO_2 planes. One possible explanation is that the Nd free spin modifies considerably the antiferromagnetic exchange interaction between the Cu ions in the CuO_2 plane, and this may destroy locally the superconductivity. A similar mechanisms has been proposed to justify the effect of Zn at Cu sites.

In summary, we performed scanning tunneling spectroscopy on high-quality YNBCO thin films and studied the effect of Nd/Ba disorder. The measurements reveal *d*-wave spectral structures that show spatial variations. At some locations on the sample surface a peak close to the Fermi energy is observed, resembling the spectra reported for BSCCO single crystals near an atomic scale impurity. The observation of such feature for the YBCO compound could be attributed to the quasiparticle resonant states at Nd substitution at the Ba site. Moreover even though all the measurements were performed tunneling along the *c* axis, the presence of a single unit-cell step is sufficient to induce a zero-bias conductance peak due to surface Andreev bound states.

We would like to thank M. Putti from the University of Genova, Italy for Hall effect measurements and J. Zasadzinski for useful discussions. This work was supported by US DOE Basic Energy Sciences—Materials Sciences under Contract No. W-31-109-ENG-38.

¹J. M. Byers, M. E. Flatté, and D. J. Scalapino, Phys. Rev. Lett. **71**, 3363 (1993).

²A. V. Balatsky, M. I. Salkola, and A. Rosengren, Phys. Rev. B **51**, 15 547 (1995).

³M. I. Salkola, A. V. Balatsky, and D. J. Scalapino, Phys. Rev. Lett. **77**, 1841 (1996).

⁴A. Yadzani, B. A. Jones, C. P. Lutz, M. F. Crommie, and D. M. Eigler, Science **275**, 1767 (1997).

- ⁵E. W. Hudson, S. H. Pan, A. K. Gupta, K.-W. Ng, and J. C. Davis, *Science* **285**, 88 (1999).
- ⁶S. H. Pan, E. W. Hudson, H. M. Lang, H. Eisaki, S. Uchida, and J. C. Davis, *Nature (London)* **403**, 746 (2000).
- ⁷A. Yadzani, C. H. Howald, C. P. Lutz, A. Kapitulnik, and D. M. Eigler, *Phys. Rev. Lett.* **83**, 176 (1999).
- ⁸Ch. Renner and Ø. Fischer, *Phys. Rev. B* **51**, 9208 (1995).
- ⁹Y. De Wilde, N. Miyakawa, P. Guptasarma, M. Iavarone, L. Ozyuzer, J. F. Zasadzinski, P. Romano, D. G. Hinks, C. Kendziora, G. W. Crabtree, and K. E. Gray, *Phys. Rev. Lett.* **80**, 153 (1998).
- ¹⁰S. H. Pan, E. W. Hudson, A. K. Gupta, K.-W. Ng, H. Eisaki, S. Uchida, and J. C. Davis, *Phys. Rev. Lett.* **85**, 1536 (2000).
- ¹¹T. Cren, D. Roditchev, W. Sacks, J. Klein, J.-B. Moussy, C. Deville-Cavellin, and M. Laguës, *Phys. Rev. Lett.* **84**, 147 (2000).
- ¹²I. Maggio-Aprile, Ch. Renner, A. Erb, E. Walker, and Ø. Fischer, *Phys. Rev. Lett.* **75**, 2754 (1995).
- ¹³H. L. Edwards, D. J. Derro, A. L. Barr, J. T. Markert, and A. L. de Lozanne, *Phys. Rev. Lett.* **75**, 1387 (1995).
- ¹⁴A. Sharoni, G. Koren, and O. Millo, cond-mat/0103581 (unpublished).
- ¹⁵N. C. Yeh, C. T. Chen, G. Hammerl, J. Mannhart, A. Schmehl, C. W. Schneider, R. R. Schulz, S. Tajima, K. Yoshida, D. Garrigus, and M. Strasik, *Phys. Rev. Lett.* **87**, 087003 (2001).
- ¹⁶J. M. Valles, Jr., R. C. Dynes, A. M. Cucolo, M. Gurvitch, L. F. Schneemeyer, J. P. Garno, and J. V. Waszczak, *Phys. Rev. B* **44**, 11 986 (1991).
- ¹⁷M. Salluzzo, A. Andreone, A. Cassinese, R. Di Capua, M. Iavarone, M. G. Maglione, G. Pica, and R. Vaglio, *IEEE Trans. Appl. Supercond.* **11**, 3201 (2001).
- ¹⁸M. Iavarone, A. Andreone, P. Orgiani, G. Pica, M. Salluzzo, R. Vaglio, I. I. Kulik, and V. Palmieri, *Supercond. Sci. Technol.* **13**, 1441 (2000).
- ¹⁹A. G. Sun, L. M. Paulius, D. A. Gajewski, M. B. Maple, and R. C. Dynes, *Phys. Rev. B* **50**, 3266 (1994).
- ²⁰M. Covington and L. H. Greene, *Phys. Rev. B* **62**, 12 440 (2000).
- ²¹S. H. Pan, E. W. Hudson, and J. C. Davis, *Rev. Sci. Instrum.* **70**, 1459 (1999).
- ²²H. L. Edwards, A. L. Barr, J. T. Markert, and A. L. de Lozanne, *Phys. Rev. Lett.* **73**, 1154 (1994).
- ²³A. T. Wu, N. Koshizuka, and S. Tanaka, *Mod. Phys. Lett. B* **13**, 735 (1999).
- ²⁴N.-C. Yeh, C.-T. Chen, G. Hammerl, J. Mannhart, A. Schmehl, C. W. Schneider, R. R. Schulz, S. Tajima, K. Yoshida, and D. Garrigus, *Phys. Rev. Lett.* **87**, 087003 (2001).
- ²⁵M. Salluzzo, A. Andreone, A. Cassinese, R. Di Capua, M. Iavarone, M. G. Maglione, G. Pica, and R. Vaglio, *IEEE Trans. Appl. Supercond.* **11**, 3201 (2001).
- ²⁶C. Panagopoulos, J. R. Cooper, T. Xiang, G. B. Peacock, I. Gameison, P. P. Edwards, W. Schmidbauer, and J. W. Hodby, *Physica C* **282**, 145 (1997).
- ²⁷Y. Tanaka and S. Kashiwaya, *Phys. Rev. Lett.* **74**, 3451 (1995).
- ²⁸H. Hancotte, R. Deltour, D. N. Davydov, A. G. M. Jansen, and P. Wyder, *Physica C* **282–287**, 1487 (1997).
- ²⁹Jian-Xin Zhu, C. S. Ting, and Chia-Ren Hu, *Phys. Rev. B* **62**, 6027 (2000).
- ³⁰H. Tsuchiura, Y. Tanaka, M. Ogata, and S. Kashiwaya, *Phys. Rev. Lett.* **84**, 3165 (2000).
- ³¹M. Salluzzo, F. Palomba, G. Pica, A. Andreone, I. Maggio-Aprile, Ø. Fischer, C. Cantoni, and D. P. Norton, *Phys. Rev. Lett.* **85**, 1116 (2000).
- ³²D. A. Bonn, S. Kamal, Kuan Zhang, Ruixing Liang, D. J. Baar, E. Klein, and W. N. Hardy, *Phys. Rev. B* **50**, 4051 (1994).